Proapoptotic Activity of New Glutathione *S*-Transferase Inhibitors

Paola Turella,[1] Claudia Cerella,[2] Giuseppe Filomeni,[2] Angela Bullo,[1] Francesca De Maria,[1] Lina Ghibelli,[2] Maria Rosa Ciriolo,[2] Maurizio Cianfriglia,[3] Maurizio Mattei,[2] Giorgio Federici,[4] Giorgio Ricci,[1] and Anna Maria Caccuri[1]

Departments of [1]Chemical Sciences and Technologies and [2]Biology, University of Rome "Tor Vergata"; [3]Department of Drug Research and Evaluation, Section of Pharmacogenetics, Drug Resistance and Experimental Therapeutics, Istituto Superiore di Sanità; and [4]Children's Hospital IRCCS "Bambin Gesù," Rome, Italy

Abstract

Selected 7-nitro-2,1,3-benzoxadiazole derivatives have been recently found very efficient inhibitors of glutathione *S*-transferase (GST) P1-1,[5] an enzyme which displays antiapoptotic activity and is also involved in the cellular resistance to anticancer drugs. These new inhibitors are not tripeptide glutathione-peptidomimetic molecules and display lipophylic properties suitable for crossing the plasma membrane. In the present work, we show the strong cytotoxic activity of these compounds in the following four different cell lines: K562 (human myeloid leukemia), HepG2 (human hepatic carcinoma), CCRF-CEM (human T-lymphoblastic leukemia), and GLC-4 (human small cell lung carcinoma). The LC_{50} values are in the micromolar/submicromolar range and are close to the IC_{50} values obtained with GSTP1-1, suggesting that the target of these molecules inside the cell is indeed this enzyme. The cytotoxic mechanism of 6-(7-nitro-2,1,3-benzoxadiazol-4-ylthio)hexanol, the most effective GSTP1-1 inhibitor, has been carefully investigated in leukemic CCRF-CEM and K562 cell lines. Western blot and immunoprecipitation analyzes have shown that 6-(7-nitro-2,1,3-benzoxadiazol-4-ylthio)hexanol promotes in both cell lines the dissociation of the GSTP1-1 in a complex with c-*jun* NH$_2$-terminal kinase (JNK). This process triggers a reactive oxygen species (ROS)–independent activation of the JNK-mediated pathway that results in a typical process of apoptosis. Besides this main pathway, in K562 cells, a ROS-mediated apoptosis partially occurs (about 30%) which involves the p38^{MAPK} signal transduction pathway. The low concentration of this new compound needed to trigger cytotoxic effects on tumor cells and the low toxicity on mice indicate that the new 7-nitro-2,1,3-benzoxadiazole derivatives are promising anticancer agents. (Cancer Res 2005; 65(9): 3751-61)

Introduction

In the last years, glutathione *S*-transferases (GSTs) have given rise to considerable interest in cancer therapy. The GSTs form a multigene family of isoenzymes, subdivided into at least 10 classes (the most abundant ones are the Alpha, Mu, and Pi classes; ref. 1). They are involved in the detoxification of cells from many endogenous and xenobiotic compounds by catalysing their conjugation to the tripeptide glutathione (GSH). Many anticancer drugs are substrates for the GST and thus they can be conjugated with the GSH and efficiently extruded from the cell by specific export pumps (2–5). Therefore, the overexpression of GSTs in the tumor cell lines, in particular of GSTP1-1, is responsible for their resistance to certain chemotherapeutic drugs (6, 7). Recently, it has been suggested the GSTs are involved in cell protection against apoptotic signals by inhibiting the stress-signaling cascade mediated by ASK1-JNK (8). In nonstressed cells, c-*jun* NH$_2$-terminal kinase (JNK) activity is efficiently inhibited by GSTP1-1 that directly interacts with JNK forming a GSTP1-1-JNK heterocomplex. UV irradiation, H$_2$O$_2$, or specific GST inhibitors have been shown to cause GSTP1-1 dissociation from the complex and an increase in the JNK activity (9, 10). For all these reasons, several attempts have been made in the past to find specific GST inhibitors to modulate the cellular resistance to anticancer drugs and enhance the cytotoxic effects of antineoplastic agents. The best characterized GST inhibitors are the diuretic ethacrynic acid and the glutathione analogue TER199 (γ-glutamyl-*S*-[benzyl]cysteinyl phenyl glycyl diethyl ester; refs. 11–18). The former (ethacrynic acid) binds to the H-site but has low affinity for the enzyme, and conjugated with GSH, it is easily excreted from the cell. Moreover, phase I clinical trials have shown severe toxicity of ethacrynic acid, including diuresis, metabolic abnormalities, and myelosuppression (7). The latter (TER 199) is a glutathione peptidomimetic which rapidly enters cells, and being a prodrug, is activated by the intracellular esterases. A different class of cytotoxic GSH analogues consists of molecules that do not inhibit GST but take advantage of its catalytic power to be activated (7, 19). An example is TER 286, whose structure has the GST binding capacity of a GSH-peptidomimetic molecule. When activated by isoenzymes of the Pi and Alpha classes, the latent cytotoxin TER 286 releases an analogue of cyclophosphamide with inherent cytotoxic activity (20).

To avoid the inconvenience of the inhibitor extrusion from the cell by specific pumps, we have recently synthesized and characterized non–GSH-peptidomimetic derivatives of 7-nitro-2,1,3-benzoxadiazole (NBD), which resulted in a strong inhibition of GSTs.[5]

In the present work, we show the cytotoxic activity of four NBD derivatives on cell lines deriving from different sources, describing in detail the apoptotic process induced by the selected derivative 6-(7-nitro-2,1,3-benzoxadiazol-4-ylthio)hexanol (NBDHEX) in human leukemic K562 and CCRF-CEM cell lines. The new GST inhibitor triggers apoptosis by the activation of the JNK/c-Jun–mediated pathway.

Materials and Methods

Cell culture and treatments. K562 (human myeloid leukemia), HepG2 (human hepatic carcinoma), CCRF-CEM (human T-lymphoblastic leukemia), and GLC-4 (human small cell lung carcinoma) cell lines were grown in RPMI 1640 supplemented with 5% FCS, 2 mmol/L L-glutamine, 100 units/mL of penicillin, and 100 mg/mL streptomycin (Sigma Co., St. Louis, MO), in a humidified 5% CO_2 atmosphere at 37°C.

NBD derivatives were synthesized as reported by Ricci et al.[5] Stock solutions of these compounds (50 mmol/L) were prepared in DMSO. Just before use, stock solutions were diluted to the appropriate concentration in RPMI cell medium with final DMSO concentration not exceeding 0.05% to 0.1%. In all experiments, control samples were exposed to requisite DMSO concentration; 0.05% to 0.1% DMSO had no cytotoxic effect.

An evaluation of cell viability at different drug concentrations was determined by sulforodamine B (SRB, Sigma) assay (21). The cells were placed in 96-well microtiter plates at a density of 1.5×10^4 cells per well, in 100 µL of medium. After 24 hours, the cells were exposed to each of the NBD derivatives under study, at the required concentration and allowed to incubate for 48 hours. After incubation, the cell growth was evaluated by an *in situ* cell fixation procedure followed by a coloring procedure with SRB capable of specifically binding to proteins.

The dose-response profile obtained fulfils the LC_{50} value (the concentration used to obtain 50% cellular mortality) for each NBD derivative assayed.

In all experiments reported later on, NBDHEX was the selected compound used to investigate the process of cell death in the leukemic CCRF-CEM and K562 cell lines.

NBDHEX was used at a concentration five times the LC_{50} value of each cell line which corresponds to 2 and 10 µmol/L for CCRF-CEM and K562, respectively. For the apoptosis studies, cells were seeded in culture flasks at 0.8×10^6 cells/mL and after 24 hours, treated with the suitable amount of NBDHEX.

Test of acute toxicity *in vivo*. The test used 25 males of the BDF1 mouse strain (18-20 g, Charles River Lab., Lecco, Italy) divided into five groups of five mice each. Three groups were treated with NBDHEX in a single administration, through i.p. injection, at the following concentrations: (a) 125, (b) 25, (c) 5 mg/kg. The remaining two groups were used as controls and were given the following: (a) olive oil vehicle containing 2.5% DMSO and (b) a physiologic solution. Mice were monitored for 15 days, providing them with food (RF-18, Mucedola, Italy) and water *ad libitum*, recording the weight variations of each mouse. Temperature (20 ± 2°C) and humidity (55% ± 5%) were continuously monitored. Treatments and experimental handling of animals were done according to the EU Directive (86/609) and Italian law (D.Lvo 116/1992). A veterinary surgeon was present to check the health status of the animals to avoid physical injury, suffering, and distress. All members of the staff involved in the experiments were trained in working with mice. At the end of this period, animals were bled under light anesthesia through the retro-orbital vein. Blood was collected in vacutainer (Becton Dickinson, Belgium) containing heparin and analyzed immediately after bleeding. The cell count was done by using hemocytometer Sysmex XT2000i (Dasit, Italy) and confirmed by microscopic analysis after May-Grumwald Giemsa staining. Mice were then humanely sacrificed and liver and spleen of each mouse were checked in terms of weight variation. Organs were 10% buffered formalin fixed for 24 hours. Samples were alcohol dehydrated and paraffin embedded. Finally, 4-µm-thick sections were H&E stained.

Enzyme activities. GST activity was measured in total cell lysates prepared as follows: cancer cell lines were collected by centrifugation at 700 × g for 5 minutes at 4°C and washed twice in PBS. Cells were resuspended in PBS and lysated by a 10-second sonication. Lysates were centrifuged at 13,000 × g for 20 minutes at 4°C and aliquots of the supernatant were used to measure the GST activity. Activity was tested spectrophotometrically at 340 nm [where the product of reaction, S-(2,4-dinitrobenzene)-glutathione, absorbs $\varepsilon = 9.6$ $(mmol/L)^{-1}$ cm^{-1}] and at 25°C, in 0.1 mol/L potassium phosphate buffer (pH 6.5), containing 1 mmol/L EDTA, 1 mmol/L GSH, and 1 mmol/l 1-chloro-2,4-dinitrobenzene (Sigma; ref. 22). One unit of GST activity is defined as the amount of enzyme catalyzing the formation of 1 µmol/min of product at 25°C.

Caspase activity was measured on K562 and CCRF-CEM cell lines treated as follows: pellets of cells obtained at different times of incubation with NBDHEX as described above, were resuspended with lysis buffer [100 mmol/L HEPES (pH 7.5), 0.1% CHAPS, 1 mmol/L EDTA, 1 mmol/L phenyl-methyl-sulfonyl-fluoride, and 10 mmol/L DTT] for 20 minutes on ice. Cells were then disrupted by a 10-second sonication. Lysates were then centrifuged at 13,000 × g for 20 minutes at 4°C and aliquots of the supernatant assayed for caspase activity with the model fluorescent peptide N-Acetyl-Asp-Glu-Val-Asp-7-amido-4-trifluoromethylcoumarin (Ac-DEVD-AFC, Sigma). Proteolytic cleavage of the peptide resulted in a fluorescence emission at 505 nm (excitation at 400 nm). As a negative control, lysates were incubated 30 minutes at 30°C with the caspase inhibitor N-Acetyl-Asp-Glu-Val-Asp-al (Ac-DEVD-CHO, Sigma) before evaluation of enzyme activity.

γ-Glutamyltranspeptidase (GGT, commercial purified enzyme from Sigma) activity was measured essentially as reported by A. Meister et al. (23) by using 1 mmol/L L-γ-glutamic acid γ-(3-carboxy-4-nitroanilide) (Sigma) and 20 mmol/L glycylglycine (Sigma) as substrates The assay was done both in 0.1 mol/L Tris-HCl buffer (pH 8.0) and in 0.1 mol/L potassium phosphate buffer (pH 6.5). The effect of NBDHEX on GGT activity was evaluated by incubating the assay solution with different concentrations of NBDHEX from 2 to 20 µmol/L, both in the absence and in the presence of 5 mmol/L GSH. γ-Glutamyl-cysteinyl-synthetase (GCS) activity was determined on cytosol from K562 cells treated with 10 µmol/L NBDHEX. At different incubation times from 15 minutes to 6 hours, cells were lysed and the supernatant was used for GCS determination essentially as previously reported (24). The effect of NBDHEX on GCS activity was also evaluated at pH 6.5 and 8.0 by adding to the assay solution different concentrations of NBDHEX from 2 to 20 µmol/L, both in the absence and in the presence of 5 mmol/L GSH.

Protein concentration was determined by the bicinchoninic acid protein assay reagent (Pierce, Rockford, IL).

Fluorescence microscopy and flow cytometry. Cells were treated for 24 hours with NBDHEX and apoptosis was detected with the fluorescence microscope by analyzing the nuclear fragmentation after staining with the DNA-specific dye Hoechst 33342 (Sigma).

The percentage of viable cells, early apoptotic and necrotic cells was determined by simultaneous staining of cells with propidium iodide (PI) and with Annexin V (Annexin V-FITC dye (Sigma). After 12 and 24 hours of treatment, cells were washed twice with cold PBS and resuspended in binding buffer (HEPES supplemented with 25 mmol/L CaCl). Cells were then incubated with Annexin V-FITC (0.5 µg/mL) and PI (2 µg/mL) for 15 minutes at room temperature in the dark. Stained cells were analyzed by a FACScalibur instrument (Becton Dickinson, San Josè, CA) as previously reported (25). The emission of unstained cells treated with NBDHEX was used as background fluorescence.

Flow cytometric data were statistically analyzed by WinMDI version 2.8 software.

Western blot analyzes. K562 and CCRF-CEM cells were treated with 10 and 2 µmol/L NBDHEX, respectively. At each time point analyzed, the cell pellet was washed in PBS and resuspended in lysis buffer containing 10 mmol/L Tris-HCl (pH 7.4), 5 mmol/L EDTA, 150 mmol/L NaCl, 0.5% IGEPAL CA-630, and protease inhibitors (Sigma). After a 30-minute incubation on ice, cells were disrupted by a 10-second sonication. Lysates were then centrifuged at 13,000 × g for 20 minutes at 4°C and supernatants were removed and stored at −80°C. Proteins (20 µg) were loaded on 10% SDS-polyacrylamide gel and transferred onto a nitrocellulose membrane (Bio-Rad Laboratories, Hercules, CA). Polyclonal anti-c-Jun and anti-JNK (1:1,000; Upstate Biotechnology, Lake Placid, NY), anti-phospho-activated c-Jun and JNK isoforms (1:500; Santa Cruz Biotechnology, Santa Cruz, CA), antiactin (1:5,000; Sigma) were used as primary antibodies. Alternatively, the cell pellet was resuspended in lysis buffer containing 62.5 mmol/L Tris-HCl (pH 6.8), 2% SDS, 10% glycerol, 50 mmol/L DTT, 0.01% bromophenol blue, and sonicated for 15 seconds to shear DNA and reduce sample viscosity. Sample (20 µg) was loaded on 10% SDS-polyacrylamide gel and transferred onto a nitrocellulose membrane. Polyclonal anti-total (Santa Cruz Biotechnology), phospho-isoform of p38^{MAPK} (Cell Signaling Technology, New England Biolabs,

Beverly, MA; 1:1,000), and antiactin (Sigma; 1:5,000) were used as primary antibodies. The specific protein complex formed upon appropriate secondary antibody (Bio-Rad) treatment (1:10,000) was identified using the "SuperSignal" substrate chemiluminescence reagent (Pierce).

Immunoprecipitation. Immunoprecipitations were done as previously described (26). Briefly, 300 μg of protein from total cell lysates were incubated in lysis buffer with 10 μL of anti-JNK antibody to a total volume of 300 μL for 2 hours at 4°C. Immunocomplexes were adsorbed with 20 μL of protein A-Sepharose for 30 minutes at 4°C. Immune pellets were boiled in SDS sample buffer. Proteins (50 μg) were loaded on 15% SDS-polyacrylamide gel and transferred to nitrocellulose. Polyclonal anti-GSTP1-1 (1:1,000; Calbiochem-Novabiochem, Darmstadt, Germany), and anti-JNK antibodies were used as primary antibodies and recognized by the "SuperSignal" substrate chemiluminescence reagent.

Tripeptide glutathione determination. To evaluate the intracellular levels of both reduced and oxidized GSH, cytosol of K562 and CCRF-CEM cells was analyzed at different times (0-8 hours) from their NBDHEX treatment. Intracellular GSH was assayed upon formation of *S*-carboxymethyl derivatives of free thiols with iodoacetic acid followed by the conversion of free amino groups to 2,4-dinitrophenyl derivatives by the reaction with 1-fluoro-2,4-dinitrobenzene (Sigma) as described by Reed et al. (27). Briefly, the cell suspension was washed with PBS, resuspended and lysated by repeated cycles of freezing and thawing under liquid nitrogen. Lysates were used for GSH/oxidized glutathione (GSSG) assay by the high-performance liquid chromatograhy technique with a NH2 BondPack column (Waters, Milford, MA), after derivatization with 1-fluoro-2,4-dinitrobenzene. Data are expressed as nmoles of GSH equivalents/mg of protein.

Detection of reactive oxygen species. Detection of intracellular ROS was done at different times from NBDHEX treatment, by a 20-minute preincubation of cells with 10 μmol/L $2',7'$-dichlorodihydrofluorescein diacetate (DCF-DA, Molecular Probes, Eugene, OR). After ROS-mediated oxidation, the $2',7'$-dichlorofluorescein becomes fluorescent and can be detected by flow cytometry after subtraction of the background fluorescence of unstained cells treated with NBDHEX.

Inhibition of the 6-(7-nitro-2,1,3-benzoxadiazol-4-ylthio)hexanol–induced apoptosis. Cells were preincubated with the antioxidant 6-hydroxy-2,5,7,8-tetramethylchroman-2-carboxilic acid (TROLOX; OXIS International, Portland, OR) 1 hour before the NBDHEX treatment. TROLOX was used at a concentration of 2 mmol/L, which under our experimental conditions, does not result in toxicity. After 1 hour from the TROLOX addition, cells were treated with NBDHEX and the time course of apoptosis was followed up to 24 hours. The effect of TROLOX on the intracellular ROS generation was determined after 20 minutes from the NBDHEX treatment (when the maximum ROS amount is detected), as reported above.

Apoptosis was also analyzed in K562 cells pretreated with 10 μg/mL of cycloeximide for 1 hour before the addition of NBDHEX to inhibit protein synthesis. Owing to the toxic effect of cycloeximide, we were unable to do experiments with CCRF-CEM.

Finally CCRF-CEM and K562 cell lines were pretreated with 20 and 30 μmol/L, respectively, of JNK inhibitor SP600125 (Calbiochem-Novabiochem) for 1 hour or with 10 μmol/L p38^MAPK inhibitor SB203580 (Calbiochem-Novabiochem) for 30 minutes before the NBDHEX addition and maintained throughout the experiment.

Data presentation. All of the experiments were repeated at least thrice. The data were expressed as mean ± SD, and significance was assessed by Student's t test. The criterion for statistical significance used was $P < 0.05$.

Results

Cytotoxic effect of new 7-nitro-2,1,3-benzoxadiazole derivatives. The cytotoxic effect of the NBD derivatives was tested on four cancer cell lines: K562 (human myeloid leukemia), HepG2 (human hepatic carcinoma), CCRF-CEM (human T-lymphoblastic leukemia), and GLC-4 (human small cell lung carcinoma).

The LC_{50} value obtained after 48 hours of treatment with each NBD derivative is reported in Table 1, showing an excellent cytotoxic activity. The LC_{50} values obtained on the four cell lines are comparable with the IC_{50} values obtained with the purified enzymatic isoform GSTP1-1.[5] To support this correspondence, the compound 6-(7-nitro-2,1,3-benzoxadiazol-4-ylamino)hexanol (compound 5 of Table 1), was tested on the various cell lines as negative control. This NBD derivative (structurally similar to NBDHEX but with the sulfur atom replaced by an amine group) does not inhibit the activity of GSTP1-1 isoform. In all the tested cancer cell lines, 50 μmol/L of 6-(7-nitro-2,1,3-benzoxadiazol-4-ylamino)hexanol, managed to easily cross the membrane; however, after 48 hours of incubation, all cancer cell lines were still viable (see Table 1). The relation between the cytotoxicity of the NBD derivatives and the GST present in the cells is further confirmed by the data obtained with the hepatic carcinoma HepG2 which seemed the most resistant to treatment with the NBD derivatives. These cells express a different GST isoenzymatic pattern compared with that of most cancer cell lines (6, 28), and the lowest GST-specific activity among the cells used in our cytotoxicity trial, as shown in Table 2.

Among the NBD derivatives tested, NBDHEX (compound 2 in Table 1) shows the lowest LC_{50} values; thus, this molecule has been selected as the model compound for this study.

Test of acute toxicity *in vivo*. To assess the acute toxicity of NBDHEX, males of the BDF1 mouse strain were treated with a single administration, through i.p. injection, with NBDHEX. The mice were followed up for 15 days and recorded for weight trend. Figure 1*A*, shows that, even after 15 days of treatment, the mice presented only slight weight variations. Moreover, each mouse's liver and spleen showed a weight within the norm and did not present postmortem abnormalities.

Histologic analysis of spleens and livers confirms the macroscopic postmortem investigation. Any toxic effect due to the NBDHEX administration was detected (see Fig. 1*B*); only a moderate liver steatosis was observed in all experimental groups, likely due to the oil vehicle because it was observed in oil and oil plus DMSO controls but not in the saline control. The RBC count showed that the treatment with NBDHEX did not change the absolute number of red cells when compared with the control. The analysis of hematocrit did not show any difference between treated animals and controls.

Interestingly, not only any cytotoxic effect was observed on WBC as shown by cell count, but a slight increase of white cells, in particular neutrophils, was observed after treatment with NBDHEX (see Fig. 1*C*), suggesting the absence of noxious effects of NBDHEX even at the maximum concentration used (125 mg/kg).

6-(7-Nitro-2,1,3-benzoxadiazol-4-ylthio)hexanol–induced apoptosis in K562 and CCRF-CEM cell lines. The mechanism of cell death was investigated in the human T-lymphoblastic leukemia CCRF-CEM and in the human chronic myelogenous leukemia K562 cell lines. The CCRF-CEM cells show the highest sensitivity towards the tested compounds, whereas K562 cells are known to be highly resistant to the induction of apoptosis by various anticancer agents (29). Evidences of apoptosis induction in K562 and CCRF-CEM cell lines by NBDHEX were obtained by measuring caspase 3 activation and by morphologic and flow cytometric analyzes.

Morphologic data were obtained by using the fluorescence microscope after nuclear staining with Hoechst 33342. Figure 2*A* shows that 24 hours of treatment of CCRF-CEM and K562 cells

Table 1. Activity trials on cell lines, LC_{50} values (μmol/L)

Compound		CCRF-CEM	GLC-4	K562	HepG2
4-(7-nitro-2,1,3-benzoxadiazol-4-ylthio)butanol	**1**	0.5 ± 0.1	3.2 ± 0.4	2.2 ± 0.2	3.2 ± 0.5
6-(7-nitro-2,1,3-benzoxadiazol-4-ylthio)hexanol	**2**	0.3 ± 0.1	1.4 ± 0.2	1.5 ± 0.1	2.9 ± 0.3
2-(7-nitro-2,1,3-benzoxadiazol-4-ylthio)imidazole	**3**	3.9 ± 0.4	10 ± 2	8.8 ± 1.1	16 ± 3
3-(7-nitro-2,1,3-benzoxadiazol-4-ylthio)propionic acid	**4**	6.5 ± 1.2	17 ± 4	38 ± 5	25 ± 4
6-(7-nitro-2,1,3-benzoxadiazol-4-ylamino)hexanol	**5**	>50	>50	>50	>50

NOTE: LC_{50} value (μmol/L) was determined by SRB assay after 48 hours from the treatment. The percentage of cell growth, obtained at different NBD derivative concentration, fulfils the LC_{50} values for each NBD derivative assayed.

with 2 and 10 μmol/L NBDHEX, respectively, induces chromatin condensation and nuclear fragmentation in small rounded bodies which represent the final steps of apoptosis (30).

In both CCRF-CEM and K562 cell lines, caspase 3 activation was readily evident 4 hours after NBDHEX treatment and its time course is similar to the apoptotic cells trend determined by Hoechst (Fig. 2*B*).

To further confirm previous results, we did cytofluorimetric analysis of cells after simultaneous staining with Annexin V-FITC and PI. After 12 hours of exposure to NBDHEX, flow cytometric analysis on K562 and CCRF-CEM cell lines showed apoptosis in about 30% of total population. At 24 hours, apoptosis further increases to a value of about 45% in both cell lines (Fig. 2*C*). The apoptotic index perfectly coincides with the morphologic and caspase activity measurements; as expected, Annexin V values are lower because the apoptotic cells in secondary necrosis were not considered. Overall, the above results clearly indicated that the NBDHEX induced cell death by apoptosis in K562 and CCRF-CEM cells and, in our experimental conditions

Table 2. Specific activity of GST (unit/mg)

Cell lines	CCRF-CEM	GLC-4	K562	HepG2
Specific activity	0.21 ± 0.03	0.35 ± 0.02	0.52 ± 0.08	0.020 ± 0.005

NOTE: GST activity was measured spectrophotometrically at 340 nm in total cell lysates as described in Materials and Methods. The enzymatic activity was normalized for protein concentration and shown as specific activity (unit/mg).
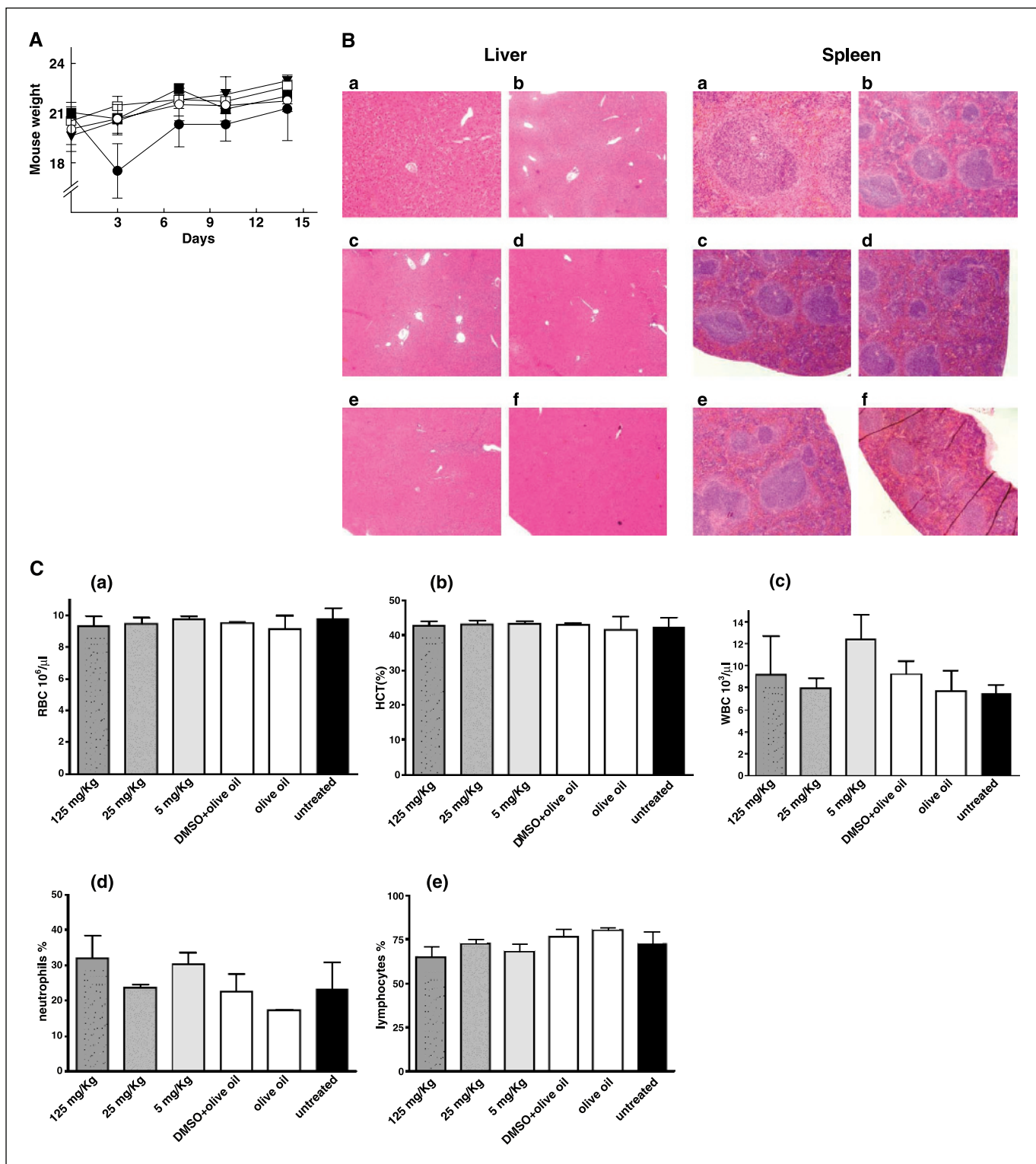
(NBDHEX used at a concentration five times the LC_{50} value of each cell line), the time course of this process was comparable in both cell lines.

Activation of the c-*jun* NH$_2$-terminal kinase/c-Jun pathway. It is known that GSTP1-1 stabilizes the inactive form of JNK by a direct interaction with this mitogen-activated protein kinase (MAPK; ref. 9). Specific inhibitors of the GSTP1-1 may induce dissociation of the JNK-GSTP1-1 complex; this is followed by activation of JNK and phosphorylation of the downstream transcription factor c-Jun (9).

To verify whether the induction of apoptosis by NBDHEX involved activation of the JNK pathway, we did Western blot analyzes of both CCRF-CEM and K562 cells after treatment with NBDHEX (Fig. 3). In both cell lines, the active phospho-JNK form was evident after 30 minutes of incubation with NBDHEX and it time-dependently increased up to 24 hours. Conversely, the phosphoactivation trend of c-Jun in CCRF-CEM cell lines showed a rapid increase after 30 minutes on NBDHEX addition, although it seemed to decrease rapidly after 3 hours of treatment, reaching the basal level after 12 to 24 hours (Fig. 3*A*). On the other hand, phosphoactivation of c-Jun in K562 cell lines parallels the activation of JNK; phospho-c-Jun was rapidly detected after 30 minutes of incubation with NBDHEX and it remained at high levels up to 12 hours (Fig. 3*B*). These data suggest that apoptosis induction was strictly associated with the activation of the JNK/c-Jun pathway even if the modality of cell response seemed different. In particular, a histotype-dependent induction of the MAPK pathway could be hypothesized.

To assess if cell treatment with NBDHEX affects the amount of the JNK-GSTP1-1 complex, K562 cells, showing very high levels of JNK in the cytosol, were subjected to immunoprecipitation analysis. K562 lysates, obtained at different times from the NBDHEX treatment, were immunoprecipitated with an anti-JNK antibody

Figure 1. Acute toxicity experiment. *A,* three groups were treated with a single administration, through i.p. injection, with NBDHEX at the following concentrations: (●) 125, (■) 25, (▼) and 5 mg/kg. The remaining two groups were used as controls and treated with the following administrations: (□) an olive oil vehicle containing 2.5% DMSO and (○) a physiological solution. Weight of each mouse was monitored for 15 days showing only slight weight variations. *B,* liver and spleen tissues, obtained after 15 days from the NBDHEX treatment, were stained with H&E. Any toxic effect due to the NBDHEX administration was detected. Liver tissues of mice treated with 125 mg/kg NBDHEX (*a* and *b*), 5 mg/kg NBDHEX (*c*), oil vehicle containing 2.5% DMSO (*d*), oil vehicle (*e*), and physiological solution (*f*). Spleen tissues of mice treated with 125 mg/kg NBDHEX (*a* and *b*), 5 mg/kg NBDHEX (*c*), oil vehicle containing 2.5% DMSO (*d*), oil vehicle (*e*), and physiological solution (*f*). *a,* magnification 10×; *b-f,* magnification 4×. *C,* hematologic variables were analyzed in mice after 15 days from the NBDHEX treatment. Absolute number of RBC (*a*) and hematocrit (*b*). WBCs are expressed as number of cells per μL (*c*); percentage of neutrophils (*d*) and lymphocytes (*e*). *Columns,* mean; *bars,* ±SD.
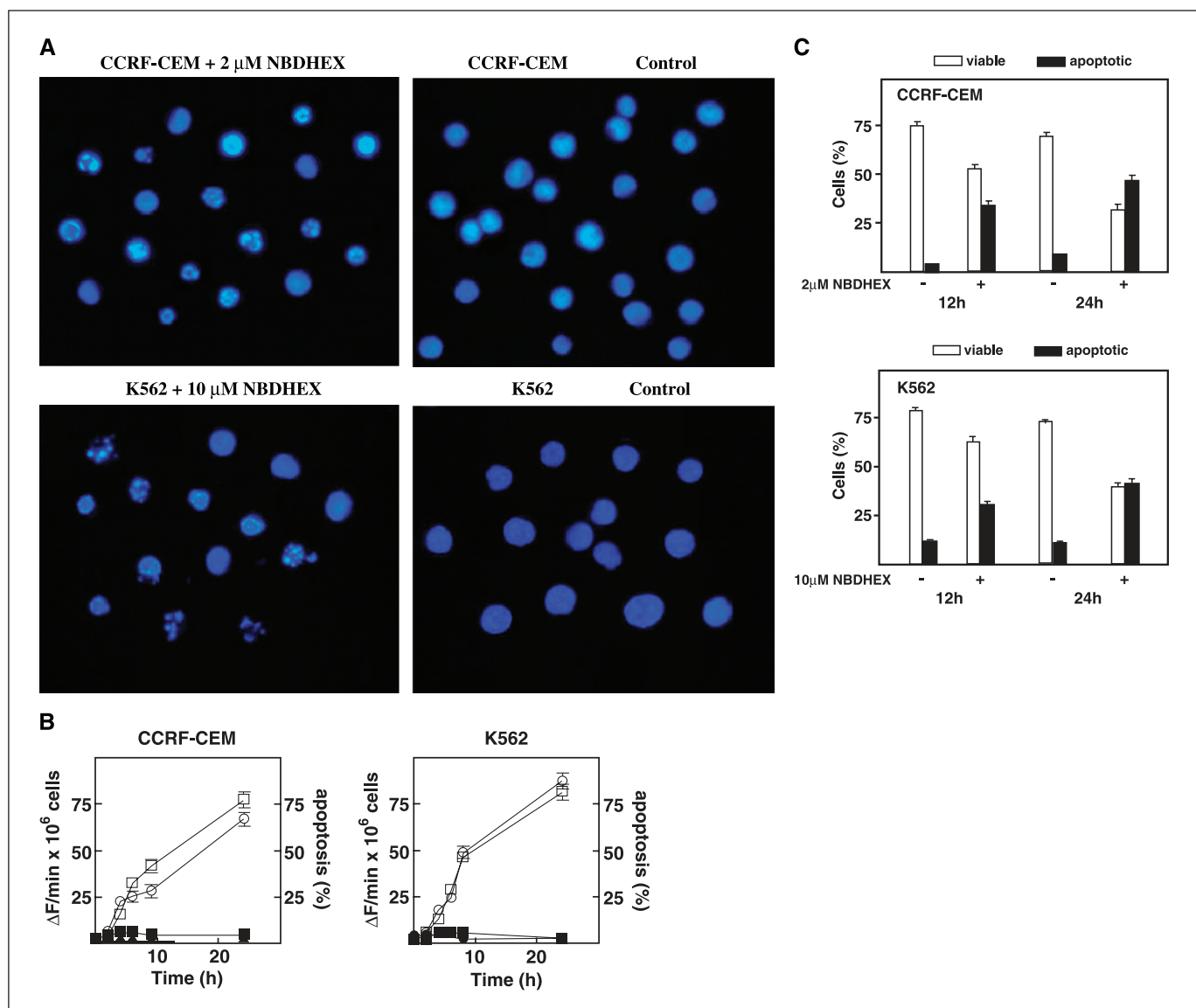
Figure 2. NBDHEX induces apoptosis in CCRF-CEM and K562 cell lines. *A,* CCRF-CEM and K562 cells, after 24 hours of treatment with NBDHEX, were stained with Hoechst 33342 and visualized by fluorescence microscopy. Pictures are a collection of cells from different fields. *B,* caspase 3 activity was determined at different times by a fluorimetric assay on cell lysates using the synthetic substrate Ac-DEVD-AFC and was compared with the time course of apoptosis determined after staining with Hoechst. Caspase activity is expressed as fluorescence change (ΔF), measured within 1 minute from the substrate addition, normalized per 10^6 cells. NBDHEX treated cells (○), untreated control cells (●). Percent of apoptosis in NBDHEX treated cells (□) and in untreated control cells (■). *C,* percentage of viable and apoptotic cells was determined by flow cytometry after simultaneous staining of cells with Annexin V/PI. Cells in secondary necrosis were not considered in the apoptotic cells quantification. NBDHEX-treated and the untreated control cells are compared at 12 and 24 hours.

and used for Western blot analysis. Figure 3*C*, shows that the amount of GSTP1-1 that coprecipitates with JNK rapidly decreased in the NBDHEX-treated cells up to 3 hours and slightly reassociated after this time even if GSTP1-1 remained at a low level when compared with control cells. These data clearly show that NBDHEX triggers the activation of the JNK/c-Jun pathway and this occurs via dissociation of the GSTP1-1 from the JNK-GSTP1-1 complex.

The involvement of the JNK/c-Jun pathway in the NBDHEX-mediated apoptosis was confirmed by the experiments carried out with the specific JNK inhibitor SP600125 (31). SP600125 (30 μmol/L) suppressed after 24 hours about 70% of the apoptosis in K562 cells treated with NBDHEX. Unfortunately, in CCRF-CEM, high SP600125 concentrations induced not negligible apoptosis in the control cells. SP600125 (20 μmol/L) suppressed >50% of

apoptosis after 24 hours with 13% of apoptosis in the control cells (Fig. 3*D*). By subtracting the contribution of apoptosis due to 20 μmol/L SP600125 alone, a net protection of about 80% can be calculated in the NBDHEX-treated cells after 24 hours. In addition, analyzing the data obtained at variable JNK inhibitor concentrations from 5 to 20 μmol/L on NBDHEX-treated CCRF-CEM, a theoretical protection from apoptosis higher than 90% can be extrapolated, at 30 μmol/L SP600125 (data not shown).

Reactive oxygen species level and redox status in cells. As previously reported, JNK dissociation from the inhibitor GSTP1-1 can be mediated by an altered intracellular redox state, in particular by ROS production (26). In fact, cytotoxic agents may generate ROS in excess of levels of the thiol buffer, and through the stress kinase cascade, they can lead to the activation of

apoptotic effector molecules. We investigated if NBDHEX was able to directly or indirectly catalyze ROS formation and the role of the ROS as potential mediators of the NBDHEX-induced apoptosis. In both K562 and CCRF-CEM cell lines, incubation with NBDHEX produced an increase of ROS with a peak value at about 20 minutes (data not shown). Preincubation of CCRF-CEM cell line with 2 mmol/L of the ROS scavenger TROLOX, resulted in a significant decrement of ROS (about 60%) in the NBDHEX-treated samples (Fig. 4*A*). However, the decrease of ROS did not affect the extent and the time course of apoptosis, suggesting that oxidative stress is not an essential event in the apoptotic

response induced by NBDHEX (Fig. 4*B*). Conversely, in K562 cells, the extent of apoptosis did not overlap that obtained in the absence of TROLOX. TROLOX (2 mmol/L) decreased the amount of the ROS by about 40% (Fig. 4*C*), and the amount of apoptotic cells proportionally decreased by about 30% after 24 hours of NBDHEX treatment (Fig. 4*D*), implying an additional role for ROS production in the NBDHEX-mediated apoptosis observed in K562 cells.

Reduced GSH is a critical component of the cellular antioxidant network, being directly involved in scavenging ROS and in maintaining intracellular thiol proteins in their reduced state. Both
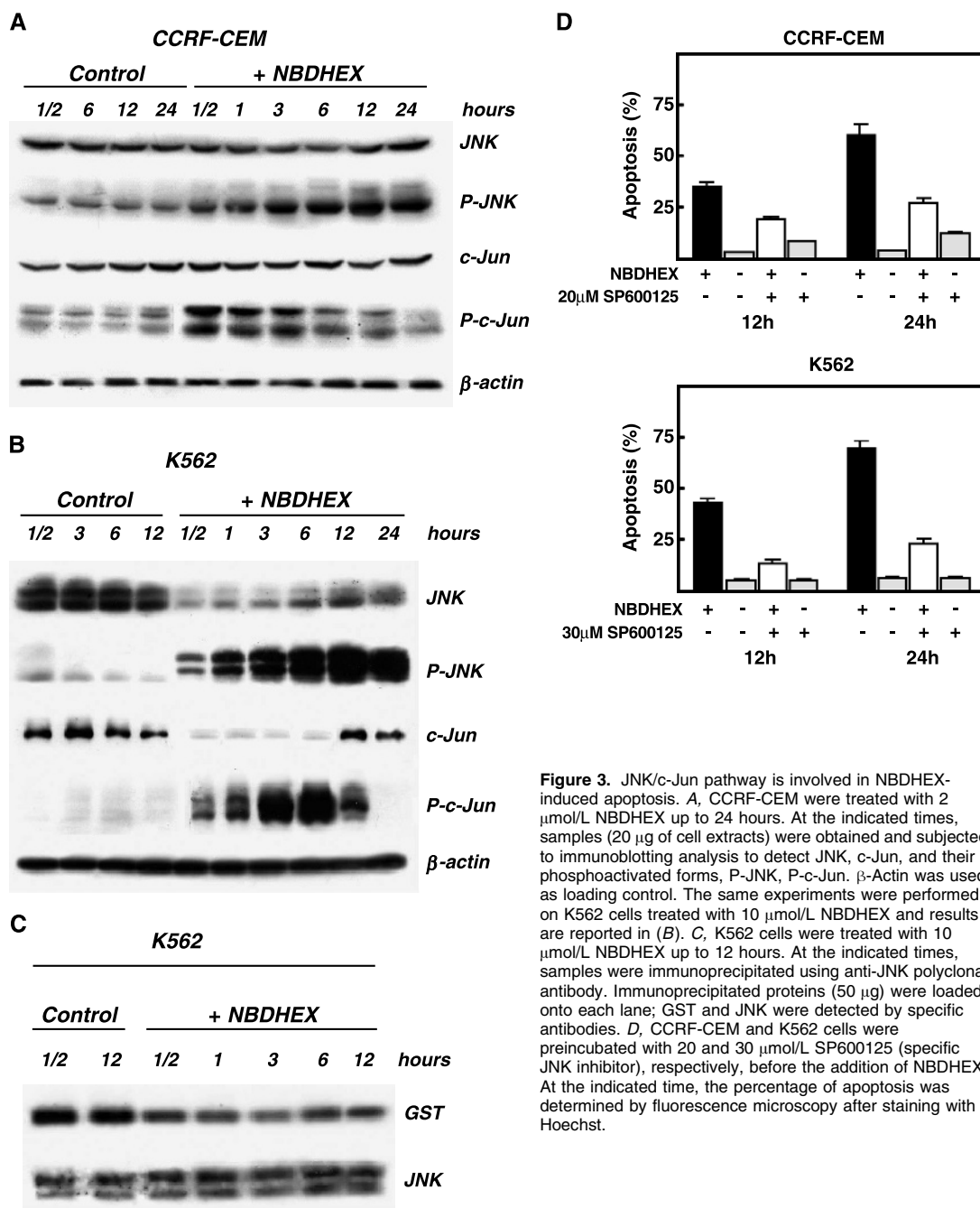

Figure 3. JNK/c-Jun pathway is involved in NBDHEX-induced apoptosis. *A,* CCRF-CEM were treated with 2 μmol/L NBDHEX up to 24 hours. At the indicated times, samples (20 μg of cell extracts) were obtained and subjected to immunoblotting analysis to detect JNK, c-Jun, and their phosphoactivated forms, P-JNK, P-c-Jun. β-Actin was used as loading control. The same experiments were performed on K562 cells treated with 10 μmol/L NBDHEX and results are reported in (*B*). *C,* K562 cells were treated with 10 μmol/L NBDHEX up to 12 hours. At the indicated times, samples were immunoprecipitated using anti-JNK polyclonal antibody. Immunoprecipitated proteins (50 μg) were loaded onto each lane; GST and JNK were detected by specific antibodies. *D,* CCRF-CEM and K562 cells were preincubated with 20 and 30 μmol/L SP600125 (specific JNK inhibitor), respectively, before the addition of NBDHEX. At the indicated time, the percentage of apoptosis was determined by fluorescence microscopy after staining with Hoechst.
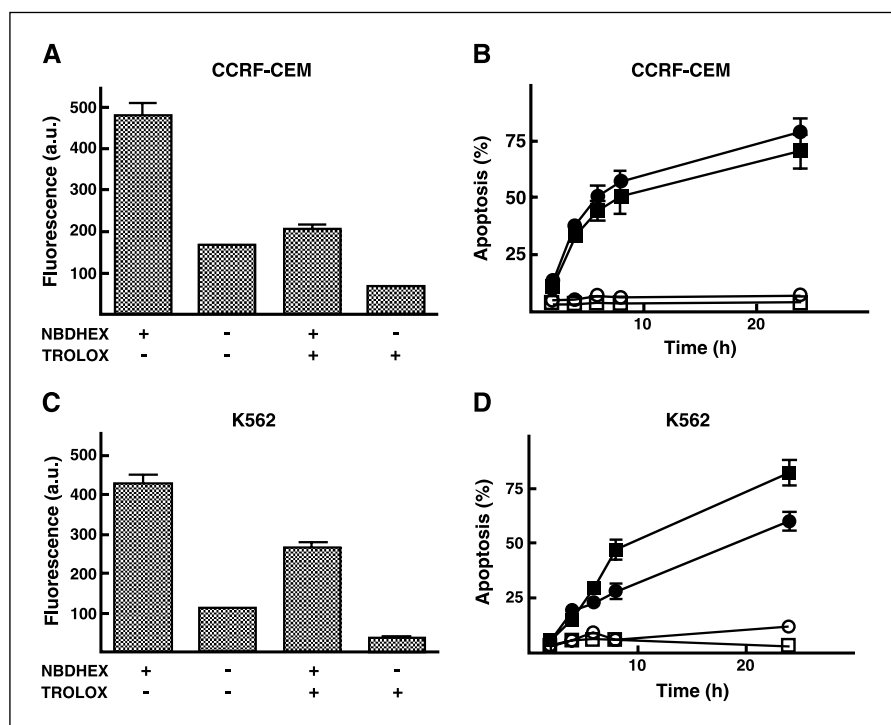
Figure 4. TROLOX partially counteracts the NBDHEX-induced apoptosis. *A,* CCRF-CEM cells were treated with 10 μmol/L DCF-DA and 2 μmol/L NBDHEX. After 20 minutes, the increase of fluorescence, due to ROS production, was detected by flow cytometry. Alternatively, CCRF-CEM cells were preincubated with 2 mmol/L TROLOX and then subjected to DCF-DA and NBDHEX treatment. *B,* time course of apoptosis of NBDHEX-treated CCRF-CEM cells in the absence (■) and in the presence of 2 mmol/L TROLOX (●); untreated control cells (□) and TROLOX-treated control cells (○). *C,* ROS amount and effect of TROLOX were determined in K562 cell line treated with 10 μmol/L NBDHEX (for experimental condition, see *A*). *D,* time course of apoptosis of NBDHEX-treated K562 cells in the absence (■) and in the presence of 2 mmol/L TROLOX (●); untreated control cells (□) and TROLOX-treated control cells (○).

GSH and GSSG concentrations remained constants in the CCRF-CEM cell line, confirming that 2 μmol/L NBDHEX treatment does not alter the thiol redox state of these cells (Fig. 5*A*). On the other hand, in the K562 cell line, 10 μmol/L NBDHEX treatment induced a small decrease of reduced GSH in the first 2 hours, accompanied by a 3-fold increase of the intracellular GSSG level (Fig. 5*B*).

The decrease of GSH observed in K562 is likely due to the formation of GSSG which can be easily extruded from the cell. Anyway possible, inhibition of NBDHEX towards two enzymes involved in the GSH homeostasis (i.e., γ-glutamyl-cysteinyl-synthetase and γ-glutamyltranspeptidase) has been evaluated. γ-Glutamyl-cysteinyl-synthetase activity was determined on K562 cells as described in Materials and Methods. Cells had a specific activity of about 1 unit/mg of protein that was not affected by the NBDHEX treatment. Moreover, NBDHEX (up to 20 μmol/L) did not affect the activity of purified γ-glutamyltranspeptidase (data not shown).

Activation of the p38 pathway. To better clarify the mechanism of K562 cell death, we used a specific inhibitor of protein synthesis. Pretreatment of K562 with 10 μg/mL of cycloeximide strongly prevented the NBDHEX-induced apoptosis (data not shown), suggesting the involvement of transcription factors in K562 cell death. A central role in the transcription factors regulation is played by MAPKs and among them p38[MAPK] senses very low changes of the intracellular redox state and may be activated by alteration of the GSH/GSSG ratio (32). Thus, we studied the effect of NBDHEX on p38[MAPK] activation. Western blot analysis clearly shows the active form of p38 in the K562-treated cells (Fig. 6*A*), whereas NBDHEX failed to induce p38 phosphorilation in K562 cells pretreated with SB203580, the highly specific inhibitor of p38[MAPK] (ref. 33; Fig. 6*B*). Conversely, the phospho-p38 is mainly undetectable in CCRF-CEM cells after 24 hours of NBDHEX treatment (Fig. 6*A*).

To establish the possible involvement of p38[MAPK] in the signaling pathway for apoptosis, K562 and CCRF-CEM cells were pretreated with p38[MAPK] inhibitor and the time course of apoptosis analyzed. After 24 hours of NBDHEX treatment, 10 μmol/L SB203580 protected K562 cells for about 30% whereas it gave a poor apoptosis suppression in CCRF-CEM cells (Fig. 6*C*).
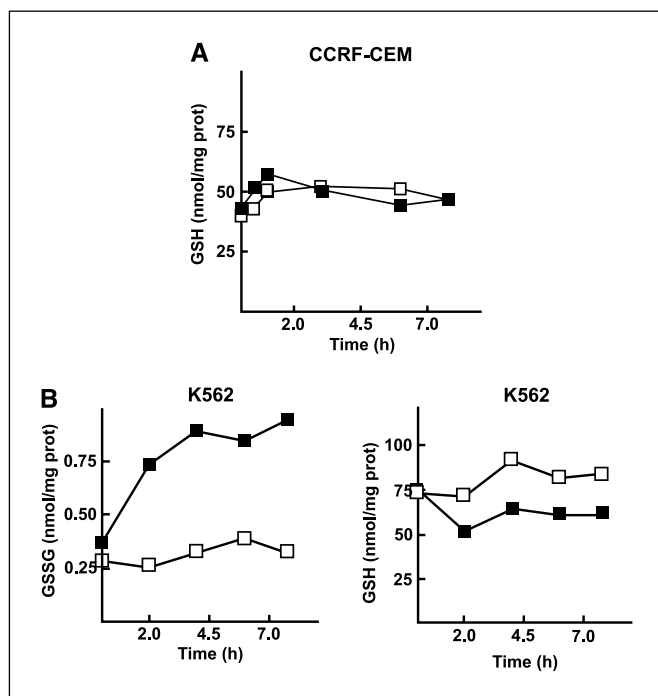

Figure 5. Redox status in cells. *A,* intracellular GSH levels were analyzed at different times (0-8 hours) in NBDHEX-treated CCRF-CEM cells (■) and in untreated control cells (□) (for conditions, see Materials and Methods). Data are expressed as nmol of GSH equivalents/mg of protein. GSSG was undetectable in our experimental conditions. *B,* intracellular GSH and GSSG levels were determined at different times (0-8 hours) in the NBDHEX-treated K562 cells (■) and in untreated control cells (□). Data are expressed as nmol of GSH (GSSG) equivalents/mg of protein.
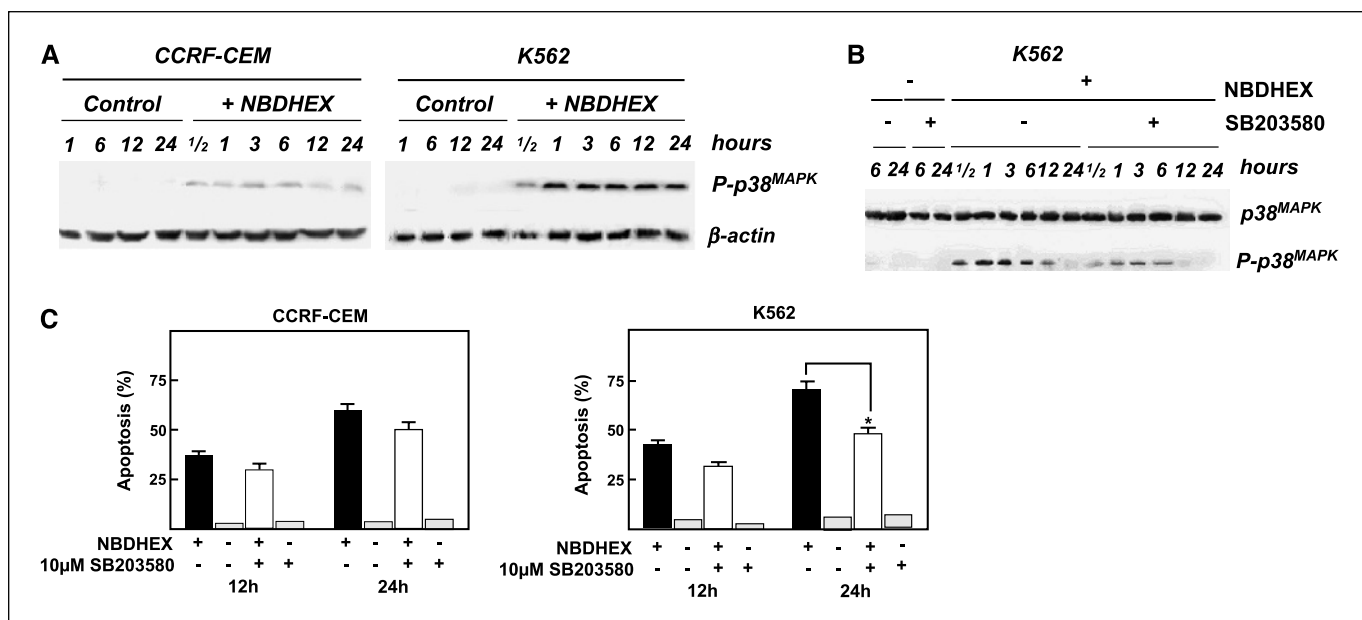
Figure 6. p38[MAPK] pathway is involved in NBDHEX-induced apoptosis. *A,* CCRF-CEM and K562 cell lines were treated with 2 and 10 μmol/L NBDHEX, respectively, up to 24 hours. At the indicated time, samples (20 μg of cell extracts) were obtained and subjected to immunoblotting analysis to detect phosphoactivated forms of p-38 (P-p38[MAPK]). β-Actin was used as loading control. *B,* K562 cells were preincubated with 10 μmol/L SB203580 (specific p38[MAPK] inhibitor) before the addition of 10 μmol/L NBDHEX. At different times, aliquots of cell suspension were withdrawn and treated for Western blot analysis to detect p-38[MAPK] and its phosphoactivated form, P-p38[MAPK]. *C,* 10 μmol/L SB203580 were added before the NBDHEX treatment and maintained throughout. At the indicate time, the percentage of apoptosis in CCRF-CEM and K562 cells was determined by fluorescence microscopy after staining with Hoechst. *Columns,* means (*n* = 3); *bars* ±SD. *, *P* < 0.05.

Overall, these data indicate that apoptosis stimulated by NBDHEX mainly involves the JNK pathway. In addition, only in K562 cells, the imbalance of the intracellular redox state may cause a partial involvement of the p38[MAPK] pathway. We cannot exclude a direct activation of p38[MAPK] by NBDHEX. However, this possibility seems unlikely because it does not occur in CCRF-CEM cells.

Discussion

In the present work, we show that new NBD derivatives, recently synthesized and characterized as very efficient inhibitors of GSTP1-1,[5] trigger apoptosis in several tumor cell lines from different sources and that this cytotoxic activity is observed at micro and submicromolar concentrations (see Table 1). The hypothesis that the binding to GSTP1-1 is a crucial step in this phenomenon is a stimulating proposal. Interestingly, the LC$_{50}$ values obtained with several cell lines are comparable with the IC$_{50}$ values obtained with the purified GSTP1-1 and this may be a first indication for a link between the cytotoxic activity of these compounds and their specific interaction with this enzyme. It is probably not casual that the higher resistance to the NBD derivatives has been observed in the HepG2 cells which display a very low GSTP1-1 expression (28). Conversely, previous studies confirm that GSTP1-1 is highly expressed in most tumor cell lines (1-30 μg/mg protein) and is also the dominant GST isoenzyme (6). The high levels of expression of this isoenzyme seem related to the proliferative capacity and to the immortalization of these cells. More recent evidences indicated a crucial antiapoptotic role of this enzyme mainly due to its noncovalent binding to JNK, an enzyme that triggers the apoptotic cascade in the cell (9). In nonstressed cells, GSTP1-1 efficiently inhibits JNK, whereas increased basal level of JNK activity is observed in fibroblasts from GSTP1-1-null mice (9). The antiapoptotic role of GSTP1-1 has been confirmed by Diederich et al. (34). These authors, inhibited the GSTP1-1 mRNA expression in K562 cells by using the natural compound curcumin and triggered 100% of apoptosis. In our conditions, the specific interaction between JNK and GSTP1-1 is likely perturbed by the presence of NBD derivatives in the cell and this may represent the crucial step of the apoptotic scenario. All results of this study can be well fitted into the tentative model of NBDHEX-induced cell death reported in Scheme 1. Briefly, NBDHEX easily crosses the cell membrane and binds to the cytosolic GSTP1-1. Binding of NBDHEX to GSTP1-1 in complex with JNK, triggers the release of GSTP1-1 from the complex leading to activation of the JNK-mediated pathway. This mechanism has been proposed previously for two GST inhibitors: the GSH peptidomimetics TER117 and TER293 that specifically bind GSTP1-1 and induce a conformational change in the enzyme promoting the dissociation of the JNK-GSTP1-1 complex. An important novelty of the present work is that a non–GSH-peptidomimetic inhibitor (NBDHEX) triggers a similar effect. It is not surprising that NBDHEX, which binds at the hydrophobic portion (H-site) of the GSTP1-1 active site,[5] behaves like the above mentioned GSH peptidomimetics that mainly interact with the GSH-binding site (G-site) of the enzyme. In fact, the mechanism of GST inhibition by NBDHEX has been recently clarified.[5] This compound is conjugated with GSH in the GST active site, leading to a σ-complex strongly stabilized by both G-site and H-site. Thus, the σ-complex may induce conformational changes in both these two subsites. The σ-complex, once in solution, easily dissociates (K_D about 10^{-2} mol/L) into NBDHEX and GSH, and this instability is a fortunate event because it avoids the excretion of the σ-complex from the cell through specific membrane pumps (multidrug resistance protein; ref. 35).
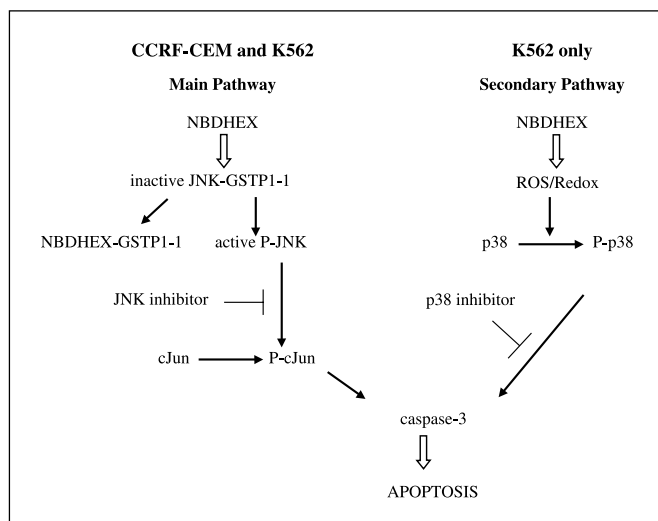
Scheme 1. Schematic model for NBDHEX-induced cell death.

We note that in both CCRF-CEM and K562 cell lines, incubation with NBDHEX produced a small increase of ROS concentration. Anyway, apoptosis seems completely ROS-independent in CCRF-CEM cells, whereas in K562 cells, the effect of TROLOX indicated that 30% of apoptosis is mediated by ROS (see Fig. 4). Moreover, the experiments done in the presence of SB203580 suggest that p38^{MAPK} was involved in the death process only in K562 cells (see Fig. 6) where we observed a concomitant alteration of the GSH/GSSG ratio which may reflect a different sensitivity of K562 cells to ROS insult. Overall, the results indicate that even in K562 cells the dissociation of the JNK-GSTP1-1 complex remains the main pathway of the NBDHEX-triggered apoptosis. The dissociation of the JNK-GSTP1-1 complex is not induced by oxidative stress but is a direct consequence of the interaction between NBDHEX and the JNK-linked GSTP1-1. Genesis of ROS in NBDHEX-treated cells and the very different

response to this stress condition of K562 and CCRF-CEM cells are unclear at the present and work is in progress to clarify these aspects.

We must underline that NBDHEX is able to induce apoptosis in the chronic myelogenous leukemia (K562) cells in spite of the presence of the apoptotic suppressor Bcr-Abl (36). The persistent activation of JNK and c-Jun observed in these cells is peculiar given the high resistance of K562 cells to the induction of apoptosis by various agents including camptothecin, 1-β-D-arabinofuranosylcytosine, etoposide, paclitaxel, staurosporine, and anti-Fas antibodies (37).

Overall the findings of this study disclose interesting perspectives of the novel NBD derivatives in the treatment of leukemia and related disorders. In the past, traditional GST inhibitors have been mainly used to prevent the multidrug resistance phenomenon in patients undergoing treatment with other chemotherapeutic agents. The NBD derivatives, besides their possible utilization in association with other chemotherapeutic agents, are themselves toxic for tumor cells. Furthermore, the tumor cells may represent the primary target of these molecules because most of these cells overexpress GSTP1-1 and this enzyme binds NBD derivatives with high affinity. The low toxicity observed *in vivo* (as deduced by the good recovery of treated mice, by the absence of histologic abnormality on liver and spleen tissues, and by the absence of cytotoxic effects on WBC and RBC) seems to confirm this idea, indicating a promising possible use of these compounds as anticancer agents. Work is in progress in our laboratory to address whether NBDHEX shows selective antitumor activity in suitable *in vivo* model systems.

Acknowledgments

References

1. Armstrong RN. Structure, catalytic mechanism and evolution of the glutathione transferases. Chem Res Toxicol 1997;10:2–18.
2. Jedlitschky G, Leier I, Buchholz U, Center M, Keppler D. ATP-dependent transport of glutathione S-conjugates by the multidrug resistance-associated protein. Cancer Res 1994;54:4833–6.
3. Ishikawa T. The ATP-dependent glutathione S-conjugate export pump. Trends Biochem Sci 1992;17:463–8.
4. Muller M, Meijer C, Zaman GJ, et al. Overexpression of the gene encoding the multidrug resistance-associated protein results in increased ATP-dependent glutathione S-conjugate transport. Proc Natl Acad Sci U S A 1994; 91:13033–7.
5. Zaman GJ, Cnubben NH, van Bladeren PJ, Evers R, Borst P. Transport of the glutathione conjugate of ethacrynic acid by the human multidrug resistance protein MRP. FEBS Lett 1996;391:126–30.
6. Tew KD, Monks A, Barone L, et al. Glutathione-associated enzymes in the human cell lines of the National Cancer Institute Drug Screening Program. Mol Pharmacol 1996;50:149–59.
7. Schultz M, Dutta S, Tew KD. Inhibitors of glutathione S-transferases as therapeutic agents. Adv Drug Deliv Rev 1997;26:91–104.

8. Townsend DM, Tew KD. The role of glutathione-S-transferase in anti-cancer drug resistance. Oncogene 2003;22:7369–75.
9. Adler V, Yin Z, Fuchs SY, et al. Regulation of JNK signaling by GSTp. EMBO J 1999;18:1321–34.
10. Wang T, Arifoglu P, Ronai Z, Tew KD. Glutathione S-transferase P1-1 (GSTP1-1) inhibits c-Jun NH$_2$-terminal kinase (JNK1) signaling through interaction with the C-terminus. J Biol Chem 2001;276:20999–1003.
11. Ploemen JH, van Ommen B, van Bladeren PJ. Inhibition of rat and human glutathione S-transferase isoenzymes by ethacrynic acid and its glutathione conjugate. Biochem Pharmacol 1990;40:1631–5.
12. Flatgaard JE, Bauer KE, Kauvar LM. Isozyme specificity of novel glutathione-S-transferase inhibitors. Cancer Chemother Pharmacol 1993;33:63–70.
13. Morgan AS, Ciaccio PJ, Tew KD, Kauvar LM. Isozyme-specific glutathione-S-transferase inhibitors potentiate drug sensitivity in cultured human tumor cell lines. Cancer Chemother Pharmacol 1996;37:363–70.
14. Ciaccio PJ, Shen H, Jaiswal AK, Lyttle MH, Tew KD. Modulation of detoxification gene expression in human colon HT29 cells by glutathione-S-transferase inhibitors. Mol Pharmacol 1995;48:639–47.
15. Tew KD, Bomber AM, Hoffman SJ. Ethacrynic acid and piriprost as enhancers of cytotoxicity in drug resistant and sensitive cell lines. Cancer Res 1988;48:3622–5.

16. Hansson J, Berhane K, Castro VM, Jungnelius U, Mannervik B, Ringborg U. Sensitization of human melanoma cells to the cytotoxic effect of melphalan by the glutathione transferase inhibitor ethacrynic acid. Cancer Res 1991;51:94–8.
17. Xu BH, Singh SV. Effect of buthionine sulfoximine and ethacrynic acid on cytotoxic activity of mitomycin C analogues BMY 25282 and BMY 25067. Cancer Res 1992;52:6666–70.
18. Nagourney RA, Messenger JC, Kern DH, Weisenthal LM. Enhancement of anthracycline and alkylator cytotoxicity by ethacrynic acid in primary cultures of human tissues. Cancer Chemother Pharmacol 1990;26:318–22.
19. Lyttle MH, Satyam A, Hocker MD, et al. Glutathione-S-transferase activates novel alkylating agents. J Med Chem 1994;37:1501–7.
20. Morgan AS, Sanderson PE, Borch RF, et al. Tumor efficacy and bone marrow-sparing properties of TER286, a cytotoxin activated by glutathione S-transferase. Cancer Res 1998;58:2568–75.
21. Skehan P, Storeng R, Scudiero D, et al. New colorimetric cytotoxicity assay for anticancer-drug screening. J Natl Cancer Inst 1990;82:1107–12.
22. Habig WH, Jakoby WB. Assays for differentiation of glutathione S-transferases. Methods Enzymol 1981;77:398–405.
23. Meister A, Tate SS, Griffith OW. γ-Glutamyl transpeptidase. Methods Enzymol 1981;77:237–53.

24. Biroccio A, Benassi B, Filomeni G, et al. Glutathione influences c-Myc-induced apoptosis in M14 human melanoma cells. J Biol Chem 2002;277:43763–70.

25. Vermes I, Haanen C, Steffens-Nakken H, Reutelingsperger C. A novel assay for apoptosis. Flow cytometric detection of phosphatidylserine expression on early apoptotic cells using fluorescein labelled Annexin V. J Immunol Methods 1995;184:39–51.

26. Filomeni G, Aquilano K, Rotilio G, Ciriolo MR. Reactive oxygen species-dependent c-*jun* NH$_2$-terminal kinase/c-Jun signaling cascade mediates neuroblastoma cell death induced by diallyl disulfide. Cancer Res 2003;63:5940–9.

27. Reed DJ, Babson JR, Beatty PW, Brodie AE, Ellis WW, Potter DW. High-performance liquid chromatography analysis of nanomole levels of glutathione, glutathione disulfide, and related thiols and disulfides. Anal Biochem 1980;106:55–62.

28. Hao XY, Castro VM, Bergh J, Sundstrom B, Mannervik B. Isoenzyme-specific quantitative immunoassays for cytosolic glutathione transferases and measurement of the enzymes in blood plasma from cancer patients and in tumor cell lines. Biochim Biophys Acta 1994;1225:223–30.

29. McGahon A, Bissonnette R, Schmitt M, Cotter KM, Green DR, Cotter TG. BCR-ABL maintains resistance of chronic myelogenous leukemia cells to apoptotic cell death. Blood 1994;83:1179–87.

30. Dini L, Coppola S, Ruzittu MT, Ghibelli L. Multiple pathways for apoptotic nuclear fragmentation. Exp Cell Res 1996;223:340–7.

31. Bennett BL, Sasaki DT, Murray BW, et al. SP600125, an anthrapyrazolone inhibitor of Jun N-terminal kinase. Proc Natl Acad Sci U S A 2001;98: 13681–6.

32. Filomeni G, Rotilio G, Ciriolo MR. Glutathione disulfide induces apoptosis in U937 cells by a redox-mediated p38 MAP kinase pathway. FASEB J 2003;17: 64–6.

33. Lee JC, Laydon JT, McDonnell PC, et al. A protein kinase involved in the regulation of inflammatory cytokine biosynthesis. Nature 1994;372:739–46.

34. Duvoix A, Morceau F, Delhalle S, et al. Induction of apoptosis by curcumin: mediation by glutathione S-transferase P1-1 inhibition. Biochem Pharmacol 2003; 66:1475–83.

35. Dietrich K. Export pumps for glutathione S-conjugates. Free Radic Biol Med 1999;27:985–91.

36. Mc Gee MM, Campiani G, Ramunno A, et al. Activation of the c-*jun* N-terminal kinase (JNK) signaling pathway is essential during PBOX-6-induced apoptosis in chronic myelogenous leukemia (CML) cells. J Biol Chem 2002;277:18383–9.

37. Kang CD, Yoo SD, Hwang BW, et al. The inhibition of ERK/MAPK not the activation of JNK/SAPK is primarily required to induce apoptosis in chronic myelogenous leukemic K562 cells. Leuk Res 2000;24: 527–34.